DEVELOPMENT OF A DISTRIBUTED MONITORING SYSTEM FOR TEMPERATURE AND COOLANT LEAKAGE

Fredrik Jensen, Eiji Takada, Masaharu Nakazawa
Hiroyuki Takahashi, Tetsuo Iguchi
Department of Quantum Engineering and Systems Science
University of Tokyo, 7-3-1 Hongo, Bunkyo-ku, 113 Tokyo, Japan

Tsunemi Kakuta
Research Group for Quantum Radiation Measurement
Japan Atomic Energy Research Institute
Tokai-mura, Ibaraki-ken 319-11, Japan

Satoshi Yamamoto
Optoelectronic Systems Laboratory, Hitachi Cable Ltd.,
Hitachi-shi, Ibaraki-ken, 319-14, Japan

Abstract

A distributed temperature sensor based on Raman scattering in optical fibres has been tested for use as a coolant loop monitor in nuclear power plants. The system has been evaluated in both gamma and neutron fields to determine system lifetime. The combined effects of temperature and radiation on the fibre sensor are demonstrated and explained. The first operational test in the experimental fast reactor Joyo is outlined.

Introduction

Present methods of coolant loop surveillance

Leakage detection and leakage monitoring in nuclear power plants are at present performed by a number of different systems and methods. Quantitative leakage determination is possible with condensate flow monitors, sump monitors and primary coolant inventory balance. However these methods are not adequate for locating leaks and are often not very sensitive [1-3]. Leak detection capabilities at particular sites exist in the form of moisture-sensitive tapes, acoustic monitoring and in some cases temperature monitoring of valves and seals. No currently employed single method combines leakage detection sensitivity, leak locating ability and leakage measurement accuracy. Information on leak location is especially scarce if the leak occurs at a point which is not specifically monitored by some means. This necessarily means that a large number of sensors need to be employed if all points of interest are to be covered. In practice, leaks are often located by visual examination after reactor shutdown. After shutdown cracks may close, which may reduce flow rates and make locating difficult. It can be concluded that a better way of detecting and locating coolant leakage could increase plant performance.

Many material investigations for nuclear power plants have pointed out that crack initiation and propagation is primarily caused by fatigue [4]. To properly estimate the thermal fatigue of coolant structure components temperature monitoring is necessary. A way of gaining this information in the most economical way possible would be advantageous for the assessment of coolant structure lifetime, again considering the actual number of sensors needed.

It is the aim of the present work to show that Raman distributed temperature sensors (RDTS) can operate in the harsh nuclear environment and thus contribute to the solution of both the above mentioned problems in reactor coolant system monitoring.

Raman temperature measurement system

The Raman temperature sensor consists of a continuous length of fibre. The location of a temperature-induced change in scattering properties is found by the propagation delay of injected laser light. The system uses the principle of optical time-domain reflectometry (OTDR) where a laser pulse (typically of 3-10 ns duration) is launched in one fibre end and the backscattered signals are then detected. This is the guided-wave optical version of the radar-location principle, and the distance, z, is related to the two-way propagation delay, $2t$, by the formula $z = tV_g$, where V_g is the group velocity of light in the fibre. The backscattered light consists of a central Rayleigh line and two Raman peaks (Stokes and anti-Stokes). Taking the ratio, R, of the anti-Stokes to Stokes intensity we obtain the temperature, T, through the expression:

$$R(T) = \left(\frac{\lambda_s}{\lambda_{as}} \right)^4 \exp\left(\frac{hc\tilde{\nu}}{kT} \right) \tag{1}$$

where λ_s, λ_{as} are the Stokes and anti-Stokes wavelengths, h is Planck's constant, c the velocity of light, $\tilde{\nu}$ the Stokes frequency shift, k Boltzmann's constant and T is the temperature. Thus by using OTDR and Raman techniques in conjunction we get both the absolute temperature and the position along the fibre.

This, then, is the principle of the measurement system used in the present work. We used a standard Hitachi FTR 030, with specifications as shown in Table 1, for our experiments. The system is comprised of an optical fibre for temperature sensing, a main measuring unit and a personal computer to display and record the temperature distribution. The system is shown in Figures 1 and 2.

Table 1. System specifications

Fibre type	Graded index (GI)	Step index (SI)
Measuring distance	2 km max.	2 km max.
Sampling distance	1 m	1 m
Distance accuracy*	±1 m	±4 m
Temperature accuracy*	±1°C	±2~4°C
Temperature resolution	0.1°C	–
Temperature range	-200~500°C (depending on fibre sheath)	
Measuring time*	90s (~9s minimum)	
Sensing fibre diameter (core/clad)	200/250 μm or 50/125 μm	
Laser wavelength	854 nm (1047 nm)	
Stokes shift	~400 cm^{-1}	
Control unit	NEC PC-9801	

(*) Measuring distance and temperature accuracy vary with measuring time, number of optical channels, etc.

Radiation effects in optical fibres

Published data on radiation effects on optical fibres show that SI fibres with nominally pure-silica cores are the most radiation resistant. Ge-doped silica-core GI fibres have been shown on numerous occasions to be inferior to pure-silica core fibres when irradiated [5]. This holds both for gamma and neutron irradiation.

The strongest radiation-induced absorption bands in the visible and near infrared spectral regions in silica arise from non-bridging oxygen holes centres (NBOHCs) at ~600-630 nm and a band-tail extending from the UV-region. This UV-tail is related to the colour centres grouped under the name E'-centres and/or directly to chlorine impurities [5,6]. Additionally peaks at 660 and 760 nm have been reported, as well as a weak "grey" absorption at longer wavelengths [7,8]. The fibre-jacket material is also of importance for the radiation response as it may embrittle during irradiation. Metal jackets are least prone to embrittlement. Polyimide jackets have a satisfactory performance in moderate radiation fields and plastic jackets are the worst performers. An additional advantage of metal jackets is their durability in high temperatures making these types of fibres good candidates for future applications at primary coolant loops.

Fibre selection

We selected a pure-silica core, polyimide-sheathed SI fibre with a core/cladding diameter of 50/125 μm and a OH-content of 30 ppm as the main fibre intended for primary loop applications. Use of Ge-doped GI fibres increase the performance (see Table 1) of the RDTS-system and thus we will use GI-fibres for secondary loop monitoring. For the highest dose-rate levels a specially developed rad-hard aluminium-jacketed fluorine-doped fibre will be employed (Table 2). To protect the fibres, steel sheaths may be employed as needed, depending on fibre type.

Table 2. Typical primary radiation levels

Location	Gamma ray (R/h)	Neutron (rem/h)	Fibre choice
Primary shield annulus	1×10^4	3×10^5	F-doped rad hard
Primary loop area:			
General area	50	0.2	Pure silica core
Contact with piping	200	–	Pure silica core
Outside loop area	0.005-0.2	0.005-0.2	Ge-doped GI

Radiation level data from Sejvar [9].

Results

Spectral data

In Figures 3 and 4 we see how the induced absorption increases with dose for the polyimide-coated pure-silica core fibre. Figure 3 shows the effect of gamma-radiation at room temperature up to a total dose of 3.7 MR. The main absorption bands are believed to comprise combinations of a strong UV-tail and NBOHCs with main absorption peaks at 600~630 nm.

Figure 4 displays absorption data taken at approximately the same dose rate as in Figure 3, however this time the temperature was ~300°C. The colour centres giving rise to the UV-tail have a weaker thermal stability than the ones related to the 600~630 nm and 660/760 nm bands. Thus the main absorption at 300°C from the visible to the near IR would be given by these thermally more stable bands. Kinetic data shown in Figure 5 indicate the induced loss to be more than 10 times lower at 300°C than at room temperature for the 800~900 nm spectral region.

System lifetime evaluation

In the section entitled *Radiation effects in optical fibres* it was argued that a limited number of absorption bands give rise to the spectra as observed in Figures 3 and 4. From Gaussian fits and literature data on these bands it is concluded that the absorption in the region 800~900 nm is given mainly by two or possibly three colour centres. A simple two-colour centre model accounts very well for the measured data and this model will therefore be used in the lifetime predictions of the RDTS system when used with

a pure-silica core fibre. Assuming the two colour-centres of the model (designated 1 and 2) to grow independently we may set up a simple growth equation for the induced loss based on saturating exponentials:

$$f = \sum_{i=1}^{2} f_i = \sum_{i=1}^{2} d\{r_i t_i (1\text{-}e^{-t/t_i})\} \tag{2}$$

where f (dB/km) is the induced loss, d (kR/h) the dose rate, r_i (dB/km/kR) a population constant and t_i (h) the relaxation time of the colour centres.

Example kinetic data from ^{60}Co-gamma-ray irradiations at room temperature at dose-rates 2.2 $\times$ 10^5 and 1.0 $\times$ 10^6 R/h, and 300°C at 1.7 x 10^5 R/h are displayed in Figure 5. The full lines are model fits. The 300°C-induced loss is a factor 10 lower than for the room temperature case. It may also be seen that there is a strong tendency for the induced loss to saturate and this pattern persists to lower dose rates.

The system lifetime, t, as a function of dose-rate, d, will be [10]:

$$t(d) = t_1 ln\left\{\frac{d(r_{1as} - r_{1s})t_1}{d[(r_{1as} - r_{1s})t_1 + (r_{2as} - r_{2s})t_2] - \Delta f}\right\} \tag{3}$$

where by system lifetime we mean the time-span in which the difference $\Delta f = f_{as} - f_s$ is smaller than some upper value. This upper value will in turn decide the effective upper temperature error $T_{err}(x)$, at every position in the fibre sensor. In equation (3) the subscripts refer to the colour centre number (1,2) and to the anti-Stokes/Stokes (as,s) parameters respectively. Obtaining model parameters from fits to the available data we get lifetime prediction curves as shown in Figure 6. We note that a maximum Δf over the lifetime of the system (> 1 year) of 0.1 dB/km is attainable up to a dose-rate of ~300 R/h for the tested fibre. The sensing fibre can also be examined for radiation damage *in-situ* by using commercial OTDR equipment at regular inspections.

Radiation-induced temperature measurement error

The temperature error, $T_{err}(x)$, produced by a given Δf is obtained from equation (1) as:

$$T_{err}(x) = T_m(x) - T_{ac}(x) = \frac{T_m^2(x)}{T_m(x) - \dfrac{10ln(e)hc\tilde{\nu}}{k\Delta fx}} \tag{4}$$

Here T_m is the measured temperature in degrees Kelvin, T_{ac} the actual experimental temperature, $\tilde{\nu}$ the Stokes-shift, h Planck's constant, c the speed of light, k Boltzmann's constant, and x the irradiated fibre length in km [10].

Under the assumption of the saturating model of equation (1) with, for example, 1000 meters of fibre being exposed to gamma radiation at a dose rate ~300 R/h leading to a maximum Δf = 0.1 dB/km we find the maximum temperature error at the end of the 1000 m fibre to be -1.9°C at 300°C. Note here that this is the maximum error along the fibre

and at, say, 10 m we only have a radiation-induced error of -0.19°C. Using a radiation-hard F-doped fibre this error would be orders of magnitude smaller. Use of the longer wavelength-laser (1047 nm) has a similar effect of reducing the temperature error by an order of magnitude.

Temperature measurements

In Figures 7 and 8 temperature data from a 335 h gamma irradiation experiment is displayed. A pure-silica core, polyimide-jacketed fibre was used and the dose-rate was $1\sim2 \times 10^2$ R/h. As predicted from equation (3) and (4) no temperature error was detected.

RDTS temperature-traces from an in-core test in the 2 kW experimental reactor Yayoi is shown in Figure 9. About 18 m of fibre was coiled and inserted into the core region. The neutron flux was $\sim10^{10}$ n/cm^2/s and the gamma dose-rate $\sim10^5$ R/h. No radiation-induced temperature error could be detected.

Temperatures up to ~300°C degrees could be measured with the polyimide-sheathed fibre with accuracies as given in Table 1, and use of Al-jacketed fibres will allow temperatures up to ~400°C to be measured.

Conclusion and future plan

The Raman distributed temperature sensor has been demonstrated to have the potential to improve coolant loop monitoring in nuclear power plants. The merits of the system include a fast time response, good locating capabilities over long distances and flexibility. With a suitable fibre/laser-wavelength choice the RDTS-system can be equipped to monitor temperature in relatively high dose rate environments at high temperatures. The upper temperature limit for these temperatures rests at ~300°C for polyimide-jacketed fibres and ~400°C for Al-jacketed fibres.

As a first operational test the RDTS-system will be installed and tested in the sodium-cooled fast 140 MWt reactor Joyo in Oarai. Both the secondary and primary loop are scheduled to be monitored by the fibre system (see Figure 10 for the primary). As the radiation level at the primary is $10^3 \sim 10^4$ R/h special radiation-hard Al-jacketed, fluorine-doped fibres will be used. In addition longer wavelength-lasers may be employed to decrease the influence of radiation.

REFERENCES

[1] D.S. Kupperman and T.N. Claytor, “Current practice and development efforts for leak detection in US reactor primary systems,” *Continuous Surveillance of Reactor Coolant Circuit Integrity*, pp. 157-164, OECD/NEA, Paris, 1986.

[2] A. Seibold, J. Bartonicek, H. Kockelman, “Operational monitoring in German nuclear power plants,” *Nuclear Engineering and Design*, Vol. 159, pp. 1-27, 1995.

[3] K. Aoki, “Reactor coolant pressure boundary leak detection systems in Japanese PWR plants,” *Nuclear Engineering and Design*, Vol. 128, pp. 35-42, 1991.

[4] R. Schiffer and M. Miksch, “FAMOS, a thermal fatigue monitoring system for sensitive locations of nuclear power plants,” *Continuous Surveillance of Reactor Coolant Circuit Integrity*, pp. 327-338, OECD/NEA, Paris, 1986.

[5] D.L. Griscom, “Radiation hardening of pure-silica-core optical fibres by ultra-high-dose γ-ray pre-irradiation,” *J. Appl. Phys*., Vol. 77, pp. 5008-5013, 1995.

[6] D.L. Griscom, “Nature of defects and defect generation in optical glasses,” *Radiation Effects in Optical Materials*, *SPIE*, Vol. 541, pp. 38-59, 1985.

[7] D.L. Griscom, “Effects of gamma and fission-reactor irradiation on the visible-range transparency of aluminium-jacketed, all-silica optical fibres with core materials fabricated by different methods,” submitted to *J. Appl. Phys*., 1996.

[8] K. Nagazawa, M. Tanabe, K. Yahagi, “Gamma-ray-induced absorption bands in pure-silica core fibres,” *Jpn. J. Appl. Phys*., Vol. 23, pp. 1608-1613, 1984.

[9] J. Sejvar, “Normal operating radiation levels in pressurised water reactor plants,” *Nuclear Technology*, Vol. 36, pp. 48-55, 1977.

[10] F. Jensen, E. Takada, M. Nakazawa, T. Kakuta and S. Yamamoto, “Distributed Raman temperature measurement system for monitoring of nuclear power plant coolant loops,” *Proceedings of SPIE* [to be published].

[11] Y. Morita, S. Yamamoto, K. Fukuchi, H. Kawakani, *DEI-93-166*, 1993 [in Japanese].

Figure 1. Principle of Raman temperature sensor

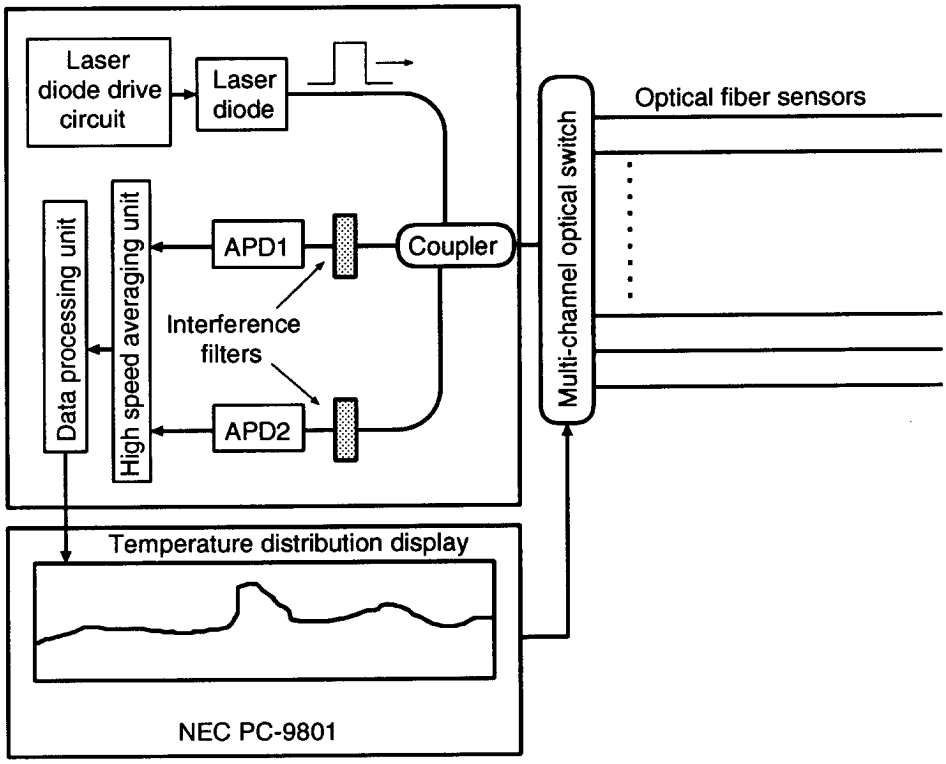

Figure 2. Raman distributed temperature measurement system

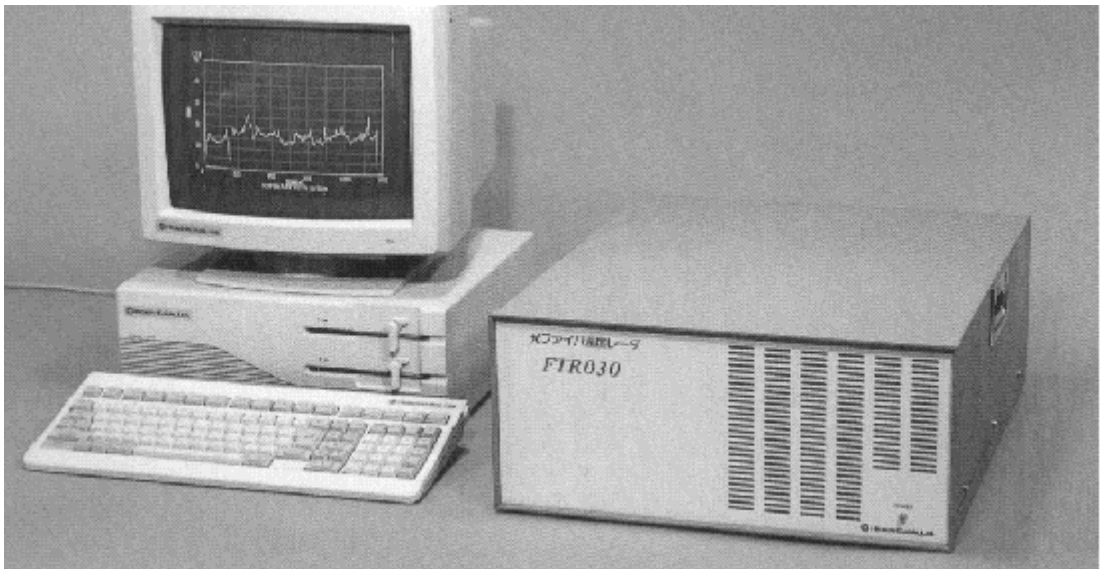

Figure 3. Gamma-ray induced loss in polyimide-coated, pure-silica core fibre at a dose rate of 2.2×10^5 R/h. Temperature ~20°C.

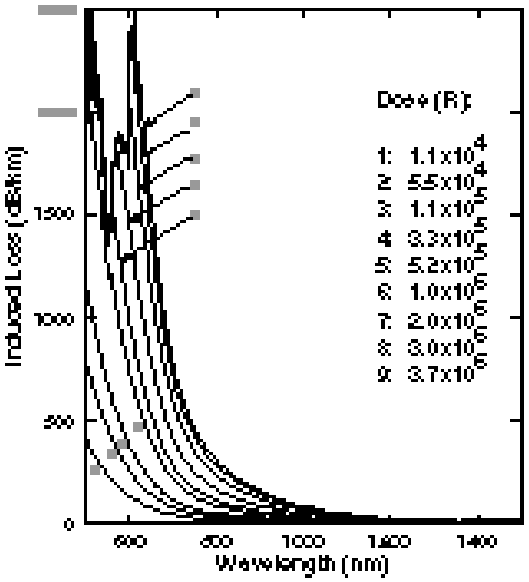

Figure 4. Gamma-ray induced loss in polyimide-coated, pure-silica core fibre at a dose rate of 1.7×10^5 R/h. Temperature ~300°C.

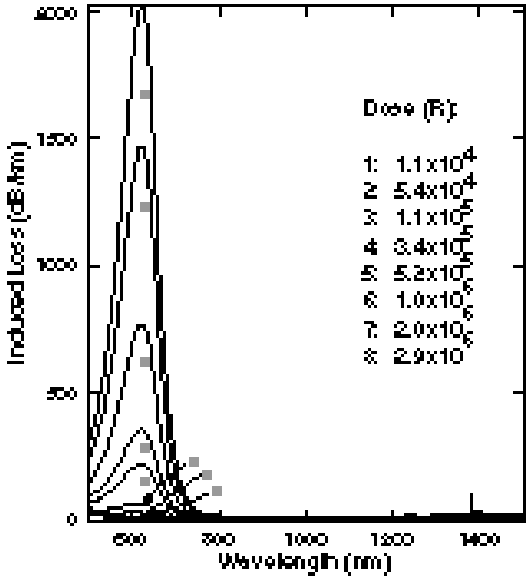

Figure 5. Example kinetic growth curves from room temperature and 300°C irradiations. Lines are model fits.

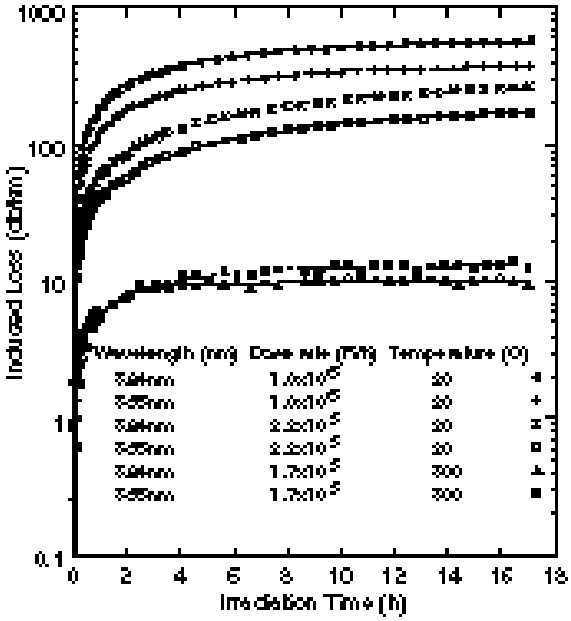

Figure 6. Lifetime extrapolations from data taken at dose rates from ~10^4 R/h to ~ 10^6 R/h.

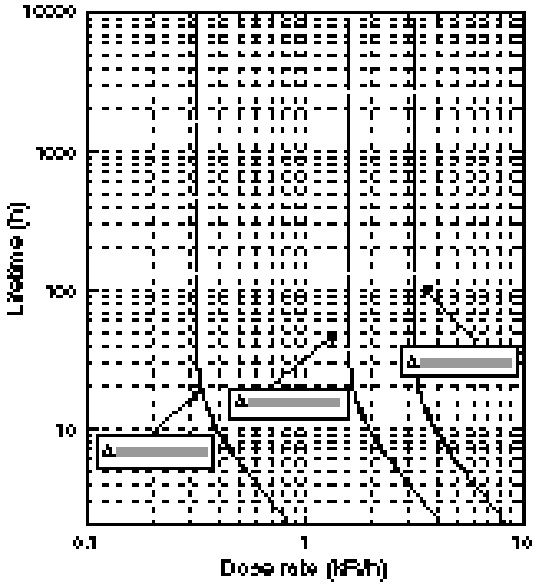

Figure 7. Temperature data taken with the RDTS-system. Before irradiation (from ref. 11)

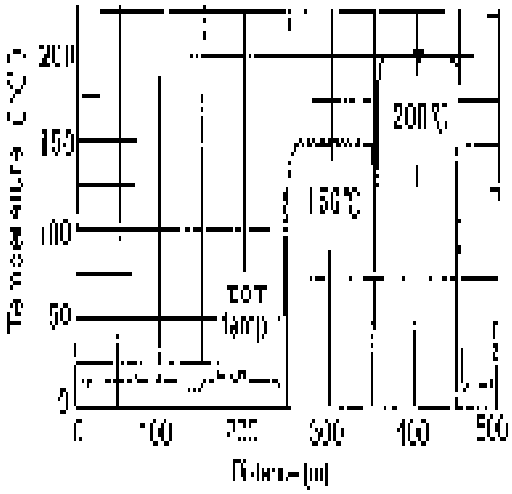

Figure 8. Temperature data taken with the RDTS-system. 335 hour irradiation at $1\sim2 \times 10^2$ R/h.

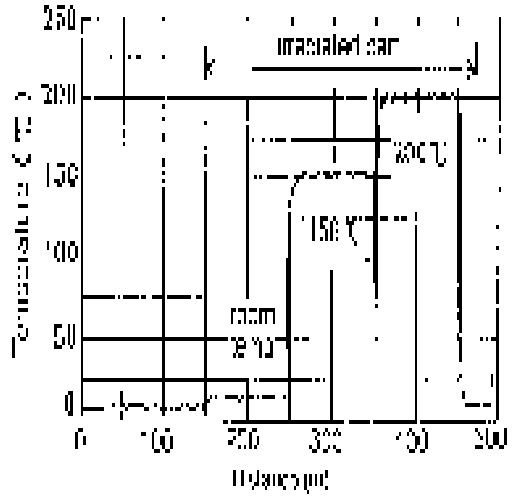

Figure 9. RDTS temperature traces at varying power levels. Core temperature was 80°C.

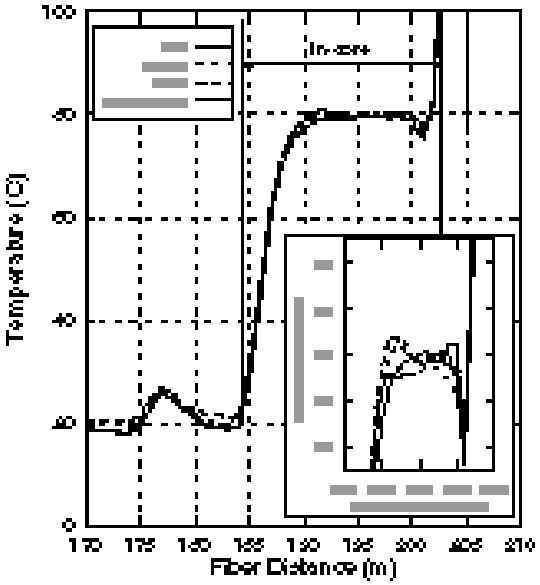

Figure 10. Primary coolant loop system of Joyo.